Chapter 1

Introduction

1.1 Summary of Introduction

In this chapter I will introduce the motivation and basic concepts that underpin this thesis. In section 1.2 I will discuss the motivations for thermoelectric materials development. In section 1.3 I will describe what the figure-of-merit zT is and explain why it is a good number for describing the performance of thermoelectric devices. In section 1.4 I will discuss the concept of Seebeck and zT enhancement via co-transport of non-electronic entropy. In section 1.5 I will discuss superionic materials and why there is so much recent interest in them as good thermoelectric materials; this section will include a brief discussion of prior work on Ag_2Se [26], Cu_2Se [23] and $Cu_{1.97}Ag_{0.03}Se$ [23]. In section 1.6 I will briefly summarize the key challenges and results of this work.

1.2 Motivation of Thermoelectric Research

A critical problem of the twenty-first century is of energy and sustainability. The limited supply of fossil fuels and the growing global population and economy have caused a steadily increasing price of electricity [37]. The massive quantities of CO_2 emitted in fossil fuel based energy production is causing worldwide climate change [152]. In order to address these challenges renewable energy sources should be developed and energy demand reduced. Though there is a pilot program to demonstrate cost ef-

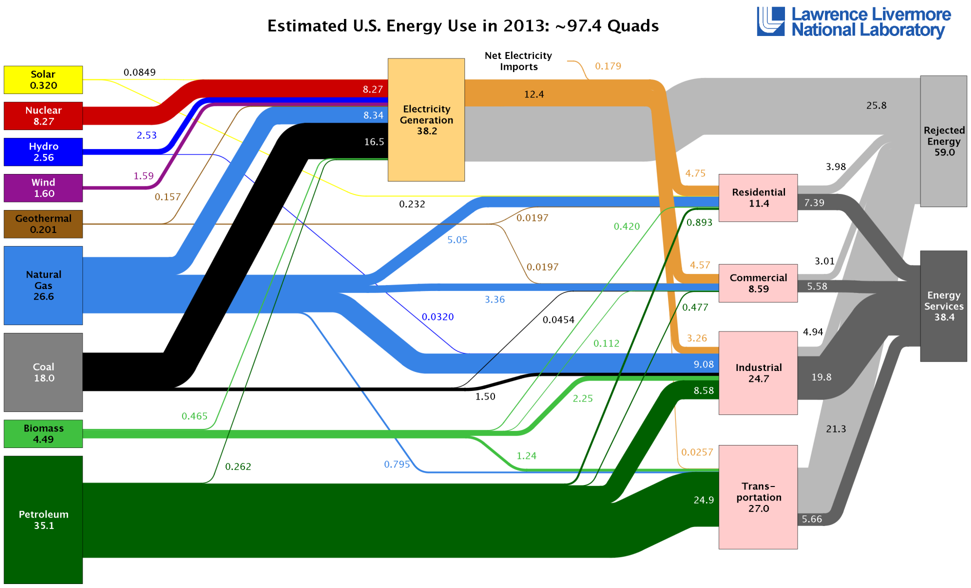

Source: LLNL 2014. Data is based on DOE/EIA-0035(2014-03), March, 2014. If this information or a reproduction of it is used, credit must be given to the Lawrence Livermore National Laboratory and the Department of Energy, under whose auspices the work was performed. Distributed electricity represents only retail electricity sales and does not include self-generation. EIA reports consumption of renewable resources (i.e., hydro, wind, geothermal and solar) for electricity in BTU-equivalent values by assuming a typical fossil fuel plant "heat rate." The efficiency of electricity production is calculated as the total retail electricity delivered divided by the primary energy input into electricity generation. End use efficiency is estimated as 65% for the residential and commercial sectors 80% for the industrial sector, and 21% for the transportation sector. Totals may not equal sum of components due to independent rounding. LLNL-MI-410527

Figure 1.1: Sankey diagram of 2013 US energy inputs and outputs. 26 Quadrillion BTU's are lost as waste head in the industrial and transportation. Over 1 Quadrillion BTU's would be recoverable with $ZT = 2$ thermolectric materials. Image credit: Lawrence Livernmore National Laboratories.

fective thermoelectric power generation [146], thermoelectric devices are principally focused on reducing demand without decreasing economic activity [13]. This is accomplished by two different strategies. The first is to develop a thermoelectric cooler that operates more efficiently than commercial refrigerants. The second is to convert waste heat directly into electricity [13].

Thermoelectric waste heat conversion is principally focused on the high temperature exhaust of industrial synthesis [76] (e.g., aluminum refining) and the medium temperature exhaust of automobiles [63]. In both these scenarios heat is rejected incidentally to the system's needs to reject the mass of the exhaust gas. Systems in which fast heat rejection or heat conservation is required are better served by heat exchange or insulation. These systems also generate heat in a manner that is geometrically inaccessible for higher efficiency heat engines based on the Rankine or Otto cycle. Thermoelectric conversion of high exergy industrial waste heat could provide approximately 10 TeraBTU/year of recovered energy in the United States alone [76].

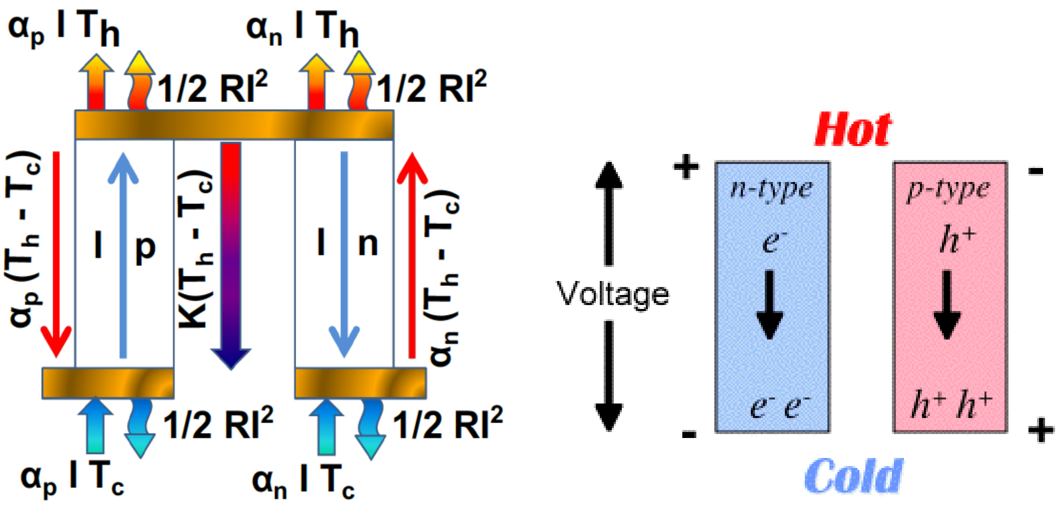

Figure 1.2: (a) Model of a thermoelectric unicouple including all electronic and thermal flows. (b) The thermoelectric effect is the result of thermodiffusion of charged carriers from the hot to cold end.

Conversion of automotive waste heat could improve fuel economy by 5% and thereby save a much larger 1 Quadrillion BTU/year [63], however device integration is more complicated due to the varied operational conditions of automobiles [104]. Therefore the typical strategy for development of thermoelectric waste heat generators is to demonstrate success in industrial applications and then integrate them into automobiles afterwards.

Thermoelectrics generators (TEGs) are compact, silent, and reliable. They are easily controlled with even simple linear PID systems [13]. For this reason they have seen use in a number of niche applications. The most important and famous of these are the Radioisotope Thermal Generators (RTGs) used to power NASA's deep space missions and its Mars Rovers [168]. In this application the compact size leads to an excellent performance on the Watts per Kilogram ratio essential for mass-limited satellite launches and the reliability ensures operation for multiple decades [202]. However, this application is not cost sensitive. Grid-scale energy conversion requires a good performance on a dollar per watt basis [203].

1.3 Thermoelectric Energy Conversion

The basic unit of a TEG is a unicouple, as depicted in Figure 1.2(a). It consists of two thermoelectric legs that are thermally in parallel and electrically in series. One of these two legs should conduct electrons (n-type) while the other conducts holes (p-type) [180]. An n-type leg will have a higher voltage at its hot side than its cold side, while the converse will be true for a p-type leg. The resulting voltage induces a current, and thereby provides power to an external load.

The voltage is induced by thermoelectric effect, as depicted in Figure 1.2(b). Charge carriers at the hot end of a material will tend to move faster and therefore diffuse quicker than species at the cold end of a material. Under a temperature gradient this results in transport to and build-up of charge carriers at the cold end of the material [67]. This process is referred to as thermodiffusion when the carriers are uncharged. In essence thermoelectric effects are thermodiffusive effects of charged particles [159]. The effects of thermodiffusion are known in a tangible sense from the transport of gas from hot regions to cold regions. The temperature gradient results in a pressure gradient and that induces a flow of particles colloquially referred to as wind.

Analogously, in a conducting material a temperature gradient induces an electrochemical potential gradient ($\tilde{\mu_e}$). That gradient in turn induces transport of particles [49]. The quantity $\frac{1}{q}\tilde{\mu_e}$ is known as the Galvani potential or voltage (V). (And not the Volta potential typically denoted by ϕ) [166]. Under open circuit operation the voltage and temperature are related by:

$$\alpha = \frac{\nabla V}{\nabla T} \tag{1.1}$$

Under closed circuit operation the voltage is diminished by the resistive flow of current. The quantity α (in many other documents denoted as S) is the *Seebeck* coefficient. Further detailed derivations of the Seebeck coefficient can be found in numerous sources [147, 32, 132, 69] Domenicali's work in particular is a detailed approach of fundamental use to anybody working on thermoelectric metrology [49]. Below I also draw strongly on Goupil *et al.*'s excellent review [69, 83].

Clearly, a large induced voltage and therefore a large α is required for a good thermoelectric material. Intuitively, the power generated will be proportional to the voltage driving it squared, and so a figure-of-merit should include a α^2 dependence. As joule heating and conduction of heat are both dissipative it can be intuited that a large electrical conductivity (σ) and a small thermal conductivity (κ) are important for good thermoelectric performance. In fact, thermoelectric materials are judged on a combination of these properties and the material temperature (T) known as the thermoelectric Figure-of-Merit (zT) [69]:

$$zT = \frac{\alpha^2 \sigma}{\kappa} T \tag{1.2}$$

But what is the meaning of zT? How does it relate to the performance of a thermoelectric as a heat engine? The answer is simple to state but will require some explanation: zT is a measure of the *thermodynamic reversibility* of a thermoelectric material acting as a heat engine [19, 187]. A similar quantity can be derived for any coupled linear energy conversion process [150]. I will first develop the zT in sketch from equilibrium thermodynamics and then develop it explicitly from non-equillibrium thermodynamics.

In 1824 Sadi Carnot proposed that there was a fundamental limit to the efficiency of a heat engine [33]. This limit depended only on the temperature at its hot and cold end. Clausius determined this efficiency, thenceforth known as the *Carnot efficiency*, to be [38]:

$$\eta_c = 1 - \frac{T_c}{T_h} \tag{1.3}$$

This limit follows directly from the second law of thermodynamics. To paraphrase Max Planck's formulation [158], "the rate of entropy production of a heat engine is always equal to or greater than zero." At the Carnot efficiency the entropy production is equal to zero. The efficiency of any heat engine is the work (dW) done divided by the heat taken from the hot end (dQ_H). The work done is the difference in the heat rejected from the hot end and the heat provided at the cold end:

$$dW \leq dQ_H - dQ_c \tag{1.4}$$

With this and the relationship between entropy and heat, $dQ = TdS$, the efficiency of any heat engine may be stated as:

$$\eta \leq 1 - \frac{T_c dS_c}{T_h dS_h} \tag{1.5}$$

The second law requirement of entropy production indicates that $dS_c \geq dS_h$ for a closed system. Therefore the limiting efficiency is η_c, as expressed in Equation 1.3. The reversibility may be defined as the ratio of entropy production required for the work done to the entropy produced dissipatively. For the perfectly reversible Carnot engine its value is infinity.

While Carnot was formulating his theory of heat engines, Thomas Johannes Seebeck was observing that by applying a temperature gradient he could deflect the needle of a compass [175, 176, 174]. A decade later Peltier determined that a current applied across the interface of a material carried a heat current [155]. William Thomson, later Lord Kelvin, integrated these effects with the nascent field of thermodynamics and postulated that the Peltier and Seebeck effect arose from the same physical effect [135]. The Seebeck coefficient was defined in Equation 1.1. The Peltier coefficient relates the reversible heat flux transported to the current applied as:

$$\pi = \alpha T = \frac{Q_R}{I}, \tag{1.6}$$

where π is the Peltier coefficient and $\pi = \alpha T$ us the first Thomson relation [135].

From these relations the reversibility of a thermoelectric material can be found. Figure 1.3 shows a simplified thermoelectric consisting of only a single leg. If the second leg is of equal and opposite Seebeck coefficient and equal σ and κ, the analysis below is excact. Suppose the leg has a resistance $R = \frac{1}{\sigma}\frac{L}{A}$ and a thermal conductance $K = \kappa\frac{A}{L}$. If it is placed under a temperature gradient and connected electrically to a

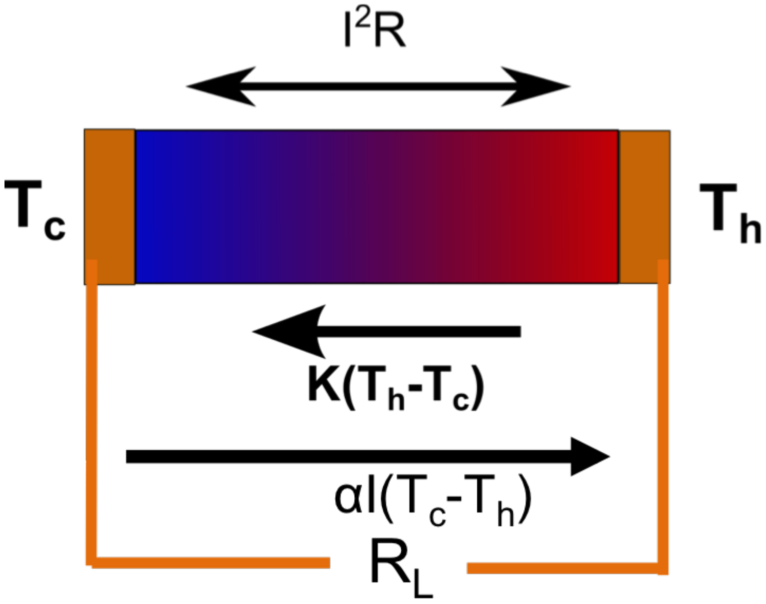

Figure 1.3: A single thermoelectric leg with all heat and thermal flows. The balance between dissipative thermal conductance and dissipative joule heating leads to constraints on the ideal geometry

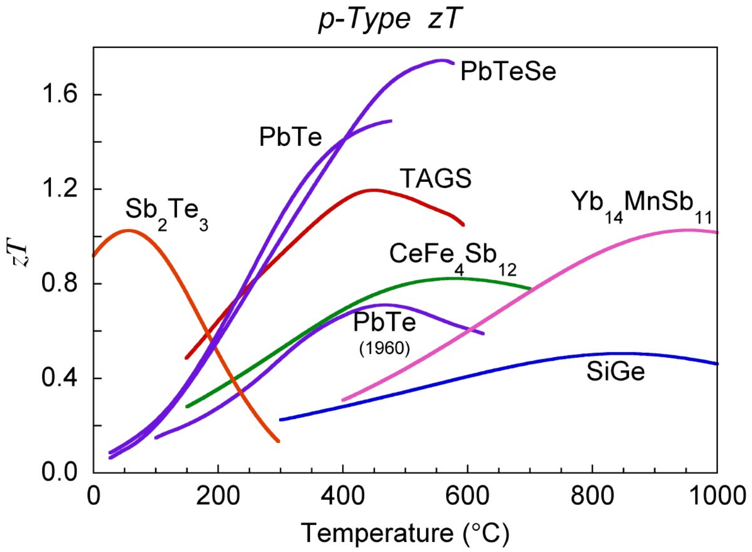

Figure 1.4: zT's for representative state of the art thermoelectric materials.

load of the same resistance, it will produce an electrical power of $V^2/R_L = \alpha^2 \Delta T^2/R$ while dissipating heat by joule heating (I^2R) and Fourier law conduction $K\Delta T$. It will transport by the Peltier effect a quantity of heat equal to the power produced.

Define the thermal conductivity under no particle flow as κ_j and that under no voltage gradient as κ_e. Then the two thermal conductivities are related by $\kappa_e = \kappa_j + T\sigma\alpha^2$. When the ratio κ_e/κ_j is maximized the work produced per heat flow is maximized. This gives:

$$\frac{\kappa_e}{\kappa_j} = \frac{\alpha^2\sigma}{\kappa_j} T + 1 \equiv 1 + zT, \tag{1.7}$$

in which maximizing zT therefore provides maximum power. Re-expressing the above as:

$$\frac{\kappa_e - \kappa_j}{\kappa_j} = zT \tag{1.8}$$

By this equation zT is the ratio of heat transformed in work by the Peltier effect to the heat that fluxes through the material. Therefore zT is a microscopic version of $\frac{dS_c dS_h}{dS_c}$ and a good representation of thermodynamic reversibility. The differential efficiency under these conditions is then:

$$d\eta = \frac{dT}{T} \frac{\sqrt{1+zT} - 1}{\sqrt{1+zT} + 1} \tag{1.9}$$

Therefore optimization of improved material zT is essential to increased device efficiency. Recent work on cost models of thermoelectric devices that includes devices costs such as a heat exchangers and metallization has shown that not only is high zT important for good device efficiency, it also is the most important factor for device cost — excepting perhaps thermoelectrics based on precious metals such as silver, gold, and rhodium. The mantra of thermoelectric material development may very well be stated as zT at any cost. [203, 117]

What are typical best values for material zT now and what values are necessary for widespread thermoelectric integration? A summary across a wide temperature range is shown in Figure 1.4; these are materials that have undergone rigorous device testing at JPL and should thus be considered as readily available for commercial

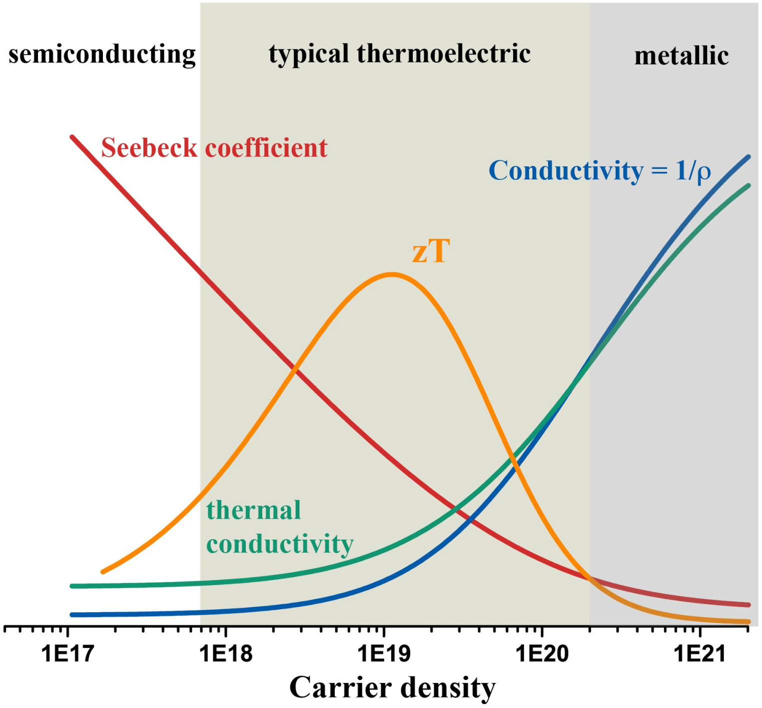

Figure 1.5: Variation of thermoelectric properties with carrier concentration as calculated with a single parabolic band model.

development. At multiple temperatures and for both charge carrier types a zT greater than unity is now available. Recent research has lead to development of materials with zT's that are potentially greater than 2, which is considered to be the threshold for device integration. While typically a publication is judged by the peak value of zT, a broad high zT across a wide temperature range is needed for commercial waste heat generation.

1.4 Entropy Co-Transport

In the previous section I defined Seebeck coefficient initially as the voltage gradient induced by a temperature gradient. However, I also noted the equivalence of the Seebeck effect and the Peltier effect that Thomson postulated and Onsager later proved explicitly from a microscopic approach based on fluctuation and dissipation. Equation 1.6 says that the Seebeck coefficient is the ratio of the reversible heat flux (Q_R) to the applied current (I) times the temperature. That is to say $\alpha = -\frac{S_R}{I}$ in which S_R is the reversible entropy flux (the minus sign is by convention). If both numerator and denominator are divided by the number of carriers transported per unit time than [49]:

$$\alpha = -\frac{S^*}{q} \tag{1.10}$$

This equation is motivated explicitly from the Onsager formalism in the appendix. In it, S^* is the entropy transported per particle — an important quantity when considering thermodiffusive transport [132] — and q is the carrier charge. The negative sign in eq 1.10 is by convention. It ensures that p-type materials have a positive Seebeck and n-type materials a negative Seebeck. Naively, one might say that what is needed is simply to increase the entropy transported per electron; just as naively one might say that one ought increase the electronic conductivity while reducing the thermal conductivity. There is no a priori relation between the transport coefficient and thus a limit on zT. However, good thermoelectric materials are heavily doped semiconductors, and the three transport coefficients are related to one another by their particular material physics [128, 154].

The transport coefficients in typical thermoelectric materials are principally related by their electronic band structure. In this work I study materials that transport thermodynamic quantities other than charge carriers and entropy, and this co-transport appears to lead to both Seebeck and zT enhancement beyond that of the band structure, and so my treatment of band structure thermoelectrics will be brief. For a more thorough discussion of band structure engineering approach to enhancing zT, the review article of Pei *et al.* [154] and the CRC chapter by Andrew May and Jeff Synder [170] are excellent resources.

It is often convenient to rewrite zT in terms of the separate contributions of electrons and lattice vibrations (phonons) to zT:

$$zT = \frac{\alpha^2\sigma}{\kappa_L + \kappa_e}, \tag{1.11}$$

in which κ_L and κ_e are the thermal conductivity contributions of the lattice and the electrons directly. The lattice thermal conductivity is purely dissipative and so ought to be minimized [180]. The lower limit of it is that due to glass-like scattering [28, 29]. An intense subject of research over the last two decades has been to devise methods of scattering phonons to reduce κ_L without scattering electrons and thereby reducing σ. Reduction of κ_e is more difficult as it is fundamentally related to the electrical conductivity by the Wiedemann-Franz Law [100]:

$$\kappa_e = L\sigma T \tag{1.12}$$

In which L is the *Lorenz number* of the material. Though the Drude model value of $L_0 = 2.44 \times 10^{-8} W \cdot \Omega \cdot K^{-2}$ is seldom exactly right, it is not violated significantly above the Debye temperature [68]. Even in very low carrier concentration samples a Lorenz number is only 60% of L_0 [154]. Both κ_e and σ should increase as carrier concentration is increased. κ_e has a weaker relationship with the Seebeck coefficient. While κ_e represents the energy conducted by the kinetic energy of electrons, the Seebeck coefficient also includes the potential energy that is transported [67]. A simple way to conceptualize the Seebeck coefficients is to divide it into two terms as per Emin [49, 61]:

$$\alpha = \alpha_{presence} + \alpha_{transport} \tag{1.13}$$

The presence Seebeck is the entropy added by adding carrier without regards to how it came to be added. The contributions from its transport through the temperature gradient (*e.g.* scattering effects are contained in $\alpha_{transport}$). While the transport term is necessary for the full derivation, the presence term is far more didactic, as it can be derived using only equilibrium thermodynamics as [169]:

$$\alpha_{presence} = -\frac{dS}{qdN}, \tag{1.14}$$

where N is the number of particles. It can be re-expressed in terms of the entropy density (s) and the carrier concentration (n) as $\alpha_{presence} = -\frac{ds}{qdn}$. The very simplest limit of this is the case in which all electron states have the same energy, *i.e.*, that the band width is small compared to k_bT. This is called the Hubbard model [14, 138]. In that case the presence Seebeck is due only to a change in entropy of mixing:

$$S_{mixing} = -Nk_b \left(c \ln(c) - (1-c) \ln(1-c) \right), \tag{1.15}$$

in which c is the concentration of carriers relative to sites. From this the Heikes formula for thermopower may be derived [135]:

$$\alpha_p = -\frac{dS}{qdN} = \frac{k_B}{q} \ln \left(\frac{c}{1-c} \right) \tag{1.16}$$

The Heikes formula gives a large magnitude of Seebeck if c is small or c is near unity. For c small the dominant carrier is electrons (n-type) and for c large it is holes (p-type). Therefore the Seebeck decreases with increasing carrier concentration. This trend is depicted in Figure 1.5, along with the corresponding trends in κ and σ. As a result of the differing carrier concentration dependence of α, κ, and σ, there is a zT peak at heavily doped carrier concentrations. A typical approach is to find a material with an electronic band structure in which the zT peak is high and attempt to dope it to the appropriate carrier concentration.

The band structure limited peak in zT only applies if electrons and heat are the only thermodynamic fluxes that show transport. Co-transport of another flux may lead to an enhancement in the entropy transported and therefore an increase in zT. Without loss of generality, let us call the additional thermodynamic flux that transports, J_m, and its corresponding equilibrium thermodynamic property, m. It will also transport entropy with quantity S_m^* per unit of m. Its thermodiffusion will have a presence contribution given by:

$$S^*_{m_presence} = \frac{dS}{dm} \tag{1.17}$$

In the presence limit the amount of m transported per a quantity of charge carrier transported is $\frac{dm}{qdN}$. Therefore the entropy co-transport provides an additional contribution to Seebeck of:

$$\Delta\alpha = -\frac{1}{q}\frac{dS}{dm}\frac{dm}{dn} \tag{1.18}$$

The additional negative sign is again due to the sign convention relating α and S^*. Though this expression in Equation 1.18 was not rigorously derived, a similar expression can determined from the Onsager phenomenological equations. From that expression Equation 1.18 can again be motivated with better grounding in non-equillibrium thermodynamics. That derivation can be found in Chapter 8.

Such entropy co-transport has been previously observed in three different types of material systems. Vibrational entropy co-transport has been observed in Boron Carbide [61, 7], lattice spin entropy co-transport has been in observed in $\mathrm{Na_xCoO_2}$ [110, 109], and lattice entropy co-transport has been observed in phonon-drag systems [148]. In the case of $\mathrm{Na_xCoO_2}$, for example, the differing spin degeneracy of electron-occupied and electron-unoccupied cobalt sites provides the mechanism for this coupling of carrier transport to entropy transport [196]. However, this strategy has thus far been limited to small changes in spin degrees of freedom of single ions; it remains an open question whether structures with more spin degrees of freedom can be coupled to charge transport.

Here we consider coupling the carrier transport to degrees of freedom associated with the entropy associated with an order-disorder phase transition. A phase transition is always associated with an entropy change because there is always a concurrent transformation in system symmetries [162]. If the entropy change of a continuous phase transition can be associated with carrier transport, a substantial enhancement in Seebeck may be obtainable. The number of degrees of freedom associated with a structural transformation scales as the number of atoms in the system rather than the number of carriers. For a typical thermoelectric material with a carrier concentration of $10^{20}\,\mathrm{cm}^{-3}$, there are 100 times as many atoms as there are charge carriers. Thus the potential Seebeck enhancement by this mechanism may be extremely large. Because phase transitions occur at a discrete temperature, it is relatively simple to distinguish the anomalous enhancement due to ordering entropy co-transport from the band structure contribution. In a material without a phase transition such enhancements may be misattributed to the band structure through incorrect determination of one of the band parameters.

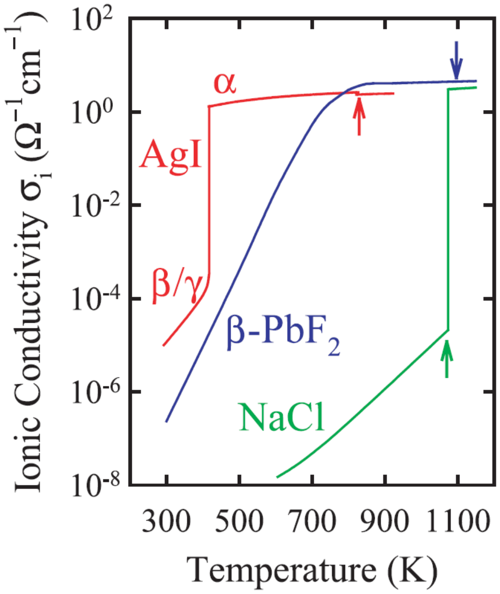

Figure 1.6: Ion conductivity of type I super-ionic AgI, type II super-ionic PbF_2, and the non-superionic NaCl. Arrow indicates the melting temperature. Superionics have a liquid-like ion conductivity while in the solid phase. Image credit to [87].

1.5 Super-ionic Thermoelectrics

Mixed ion-electron conductors are of recent and increased interest as thermoelectric materials. Though there is long-standing work on the Zn ion conductor Zn_4Sb_3 [204], recent results have sparked interest in mono-valent coinage metal chalcogenides such as Ag_2Se [136, 64, 199, 133], Ag_2Te [50, 178], and Cu_2Se [84, 122]. These materials all have ion conductivity greater than 1 S/cm at elevated temperatures [21, 87], which qualifies them phenomenologically as super-ionic conductors as defined by Rice and Roth [163]. This is a classification rather than a definition and so it is not held uniformly. Sometimes a material with ion conductivity one to three orders of magnitude smaller is called super-ionic due to its resemblance in structure and behavior to canonical super-ionics. The ion conductivity of 1S/cm is similar to that of a molten salt [87, 70, 34]. For this reason the super-ionic materials are often spoken of as having a molten sublattice. For example, in the Ag^+ conductor AgI the I^- are taken to be in a rigid cage, while the Ag^- is free to travel [97].

Why are these materials of such interest as thermoelectrics? Because their lattice thermal conductivity is extremely low. For example, in $Ag_2Se_{0.05}Te_{0.05}$ it is only 0.5 W/mK at 400 K [50] and Ag_8GeTe_6 has been reported as having a lattice thermal conductivity of $0.25W/mK$ at $300K$ with only negligible contribution from electrons. This thermal conductivity is almost certainly at or below the glassy limit proposed by David Cahill.

Super-ionics were divided into three categories by Pardee and Mahan [151] based on the manner by which the super-ionic state is achieved. Their classification system superceded an earlier system based on chemical composition and structure instead of phenomenological behavior. The dependence of ionic conductivity on temperature is plotted for prototypical members of each superionic classification in Figure 1.6. In type I superionics such as AgI [97], the ionic conductivity increases suddenly at a phase transition temperature. In type II superionic such as PbF_2 [86], the ionic conductivity increases continuously but super-exponentially to a phase transition temperature. Type III super-ionics such as $Na - \beta - Al_2O_3$, the ionic conductivity increases according to an Arrhenius behavior with no phase transition.

The super-ionic phase transition is of particular interest to this study. Type I and type II super-ionic conductors are characterized by a structural phase transition with an entropy change close to that of melting (*i.e.*, order $10\,\mathrm{J} \cdot \mathrm{K}^{-1} \cdot \mathrm{mol}^{-1}$) and a concurrent increase in ion conductivity [151]. For type I super-ionic conductors there is a sudden enthalpy release at the phase transition temperature (*i.e.*, a first order phase transition) and a concurrent discontinuous increase in ionic conductivity. For type II super-ionic conductors the ionic conductivity increases super-exponentially up to the phase transition temperature, the structure changes continuously, and there is a lambda-shaped peak in heat capacity like that characteristic of a second order phase transition [87]. In the final chapter of this work I will show that Ag_2Se is a type I super-ionic, while Cu_2Se is a type II super-ionic. This difference is essential to understanding their behavior in their ordered phases just below their respective super-ionic phase transitions.

1.6 Key Challenges and Results

Having outlined the motivations for this study, I should also present a brief outline of the thesis. In the course of thesis I had to overcome a number of challenges in order to come to my conclusions, and I had to develop a broad theoretical understanding to interpret my data. I needed to measure the chemical and transport properties of these materials, see Chapter 2. Metrology of the Seebeck coefficient near phase transitions was a particularly challenging part of the work for which new methodology was developed, see Chapter 3. The most common question I faced with respect to the applicability of my work to real thermoelectric device was whether ion conducting materials would be stable under applied current. In Chapter 4 I examine this question both by a review of a past attempt by JPL and the DOE to use $\mathrm{Cu_{1.97}Ag_{0.03}Se}$ as a super-ionic material and through experimental tests designed to simulate device conditions. Determination of the nature of the phase transition is particularly important to this work. In the course of this work we proved that contrary to all previously published literature, Cu_2Ses phase transition is second order not first order, see Chapter 5. This understanding was crucial to calculating correctly its zT. In Chapter 6 I report my data and analysis of the transport behavior of $\mathrm{Ag_2Se}$. I also give an overview of why super-ionics are of interest as thermoelectrics and of band structure modeling of thermoelectrics. In Chapter 7 I introduce the concept of entropy co-transport as means of enhancing thermoelectric performance, and I present the transport data and analysis of both $\mathrm{Cu_2Se}$ and $\mathrm{Cu_{1.97}Ag_{0.03}Se}$. In the final chapter I integrate my results and a full phenomenological explanation of the thermoelectric enhancement of $\mathrm{Ag_2Se}$ and $\mathrm{Cu_2Se}$. From the basis of this hypothesis a series of future experimental goals are proposed.